Eur. Phys. J. D **35**, 411–416 (2005)
DOI: 10.1140/epjd/e2005-00191-8

THE EUROPEAN PHYSICAL JOURNAL D

Elastic scattering of electrons from tetrahydrofuran molecule

A.R. Milosavljević[1], A. Giuliani[2,a], D. Šević[1], M.-J. Hubin-Franskin[2,b], and B.P. Marinković[1,c]

[1] Institute of Physics, Pregrevica 118, 11080 Belgrade, Serbia and Montenegro
[2] Laboratoire de Spectroscopie d'Électrons Diffusés, Université de Liège, Institut de Chimie, Bâtiment B6c, 4000 Liège, Belgium

Received 12 April 2005 / Received in final form 26 May 2005

Abstract. Absolute differential cross-sections (DCSs) for elastic scattering of electrons from the DNA backbone sugarlike analogue tetrahydrofuran (THF) molecule were determined using a crossed beam measurements for incident energies from 20 eV to 300 eV and scattering angles from 10° to 110°. Using the relative-flow technique, elastic DCSs for THF relative to nitrogen have been obtained at incident energies of 20, 30, 40, 50 and 60 eV. In the energy region above 30 eV, the DCSs were measured independently as a function of both incident electron energy and scattering angle. Therefore, this set of relative DCSs has been calibrated to the absolute scale via normalization to a single point in the overlapping region. Additionally, both vibrational and electronic energy loss spectra for THF are presented and influence of energy resolution to the obtained DCSs is discussed.

PACS. 34.80.Bm Elastic scattering of electrons by atoms and molecules

1 Introduction

It is well-known that a large amount of energy deposited in living cells by ionizing radiation is channelled into the production of low-energy secondary electrons. Therefore, investigation of radiation damage in living tissue upon exposure to high-energy radiation must include and apprehend these subsequent processes describing reactions between secondary electrons and cell constituents. In a recent paper [1], dissociation of small DNA's basic components as a function of incident energy of bombarding electrons has been shown to correlate to the measured DNA damage. Being a simple prototype to investigate electron-induced decomposition of deoxyribose ring (see Fig. 1), tetrahydrofuran (THF) molecule (C_4H_8O) has revived a quite deal of interest in radiation damage research in a few recent years. Several papers on electron interaction with either gaseous or surface deposited THF have been recently published, which consider electron spectroscopy of resonance-enhanced vibrational excitations [2], electron-stimulated desorption yields of H^- from thin films [3,4] and electron-induced damage of solid THF films [5]. In the latest paper [5], the earlier work on THF has been summarized, as well. However, according to our knowledge, there are no published absolute differential cross-sections (DCSs) for elastic scattering of electrons by gaseous THF. This cross-section data set would be of interest in estimating and modelling of products production processes induced by electrons within a molecular sample. In particular, the electron scattering cross-sections, both differential and integral, are the input parameters for energy deposition modelling that is based on a Monte Carlo simulation of the single electron scattering process [6,7].

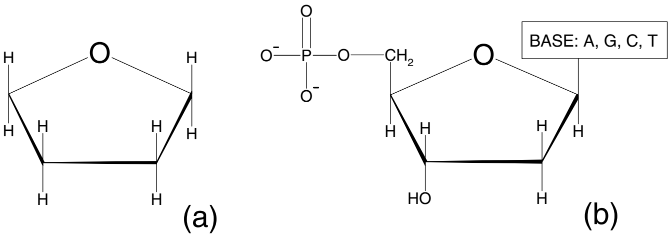

Fig. 1. Schematic drawing of (a) tetrahydrofuran (THF) molecule (C_4H_8O), and (b) the monomer unit of DNA (nucleotide) that consists of deoxyribose sugar, a base (adenine, guanine, cytosine, thymine) attached to the sugar, and a phosphate group.

In the present paper, we report a comprehensive set of DCSs for elastic electron-THF scattering that covers large energy range from 20 eV to 300 eV and has been obtained using two different crossed beam spectrometers, respectively with high (30–50 meV) and low (0.5–1 eV) energy resolution. At low incident electron energies, the absolute DCSs were obtained according to relative-flow technique. These absolute values were then used to normalize relative

---

[a] *Present address*: Laboratoire de Spectrométrie de Masse, ICSN-CNRS, avenue de la Terrasse, 91190 Gif/Yvette, France.
[b] Directeur de recherche F.N.R.S.
[c] e-mail: `bratislav.marinkovic@phy.bg.ac.yu`

DCSs at higher energies according to separate direct measurements of both angular and energy dependencies. The experimental procedure has been checked according to DCS measurements for nitrogen and krypton.

2 Experiment

The experimental results were obtained on two different apparata, one placed in Liège and the other in Belgrade. The Liège apparatus consists of a Vacuum Generator SEELS 400 electron spectrometer, modified for work on gaseous targets and described previously [2,8]. Briefly, it includes an electron gun followed by a monochromator, an electron energy analyzer and a channel electron multiplier as a detector. Both monochromator and analyzer are 150° hemispherical electrostatic type and are fitted with three aperture electrostatic zoom lenses. The effusive molecular beam is formed using the stainless steal needle with 1 mm internal diameter and 136.5 mm length, placed perpendicularly to the incident electron beam. Intensity of the incident beam current, as monitored using a rotatable Faraday cup, was about 5×10^{-10} A. The analyzer can be rotated around the molecular beam in the range 0° to +110°. The operating pressure ranged from about 6×10^{-6} to 2×10^{-5} mbar and the base pressure was better than 1.0×10^{-8} mbar (obtained with a cryogenic pump). The angular resolution was investigated earlier and was found to be better than ±2°. The incident energy scale was calibrated to ±12 meV with respect to the oscillations in the elastic decay channel of the lowest-energy shape resonance in N_2 (see [2], and references therein). All measurements were made at constant pass energy mode with a resolution of the 35–40 meV (Full Width at Half Maximum of the elastic peak) and with 8 or 10 meV steps. The anhydrous THF was purchased from Aldrich Chemical Ltd. with a stated purity of +99% and was used after several cycles of freeze-thaw under vacuum.

The relative flow apparatus is composed of two separate introduction lines for the sample and the reference to avoid cross contaminations. Each line is fitted with an MKS mass flow meter coupled with a precision gas flow valve, allowing us to accurately control and record the mass flows into the vacuum chamber. The system is pumped by a turbomolecular pump, which gives residual pressure of 5×10^{-6} mbar, as monitored by a Penning gauge, which allowed precise determination of the zero of flow meters. The absolute pressure of the introduction lines (head pressure), i.e. before the needle, was monitored by a capacitance gage.

The relative elastic differential cross-sections (DCSs) have been measured by recording the elastically scattered electron signal (elastic peak) of THF at each angle and energy of interest. The effective path length correction was obtained according to elastic DCS for nitrogen, which was measured under the same experimental conditions as for THF for each incident energy and compared to existing data [9].

In order to normalize the elastic relative DCS, the absolute values of the elastic DCS of THF have been measured up to 60 eV and at 10°, 20° and 30° using the relative flow method and with nitrogen as the reference gas. The relative flow method is based on the determination of the ratio of elastic cross-section of the gas under study (X) to the known absolute elastic cross-section of a reference gas (*ref*) at a given energy (E) and scattering angle (θ). The procedure has been described elsewhere [8] and is therefore shortly described in the following. This method requires measurements of the ratio of the elastically scattered intensity $N_e(E,\theta)_X / N_e(E,\theta)_{ref}$. When this ratio is determined at a constant impact electron current, transmission function of the analyzer and scattering angle, it can be expressed as:

$$\frac{N_e(E,\theta)_X}{N_e(E,\theta)_{ref}} = \frac{DCS_{elas}(E,\theta)_X}{DCS_{elas}(E,\theta)_{ref}} \frac{\int_r [\rho(r)]_X}{\int_r [\rho(r)]_{ref}} \tag{1}$$

where $\rho(r)$ represents the spatial distribution of the molecular beams density and $DCS_{elas}(E,\theta)$ is the elastic cross-section. Therefore, in order to determine the DCS, knowledge of the density distributions of the target to reference gas is required. It has been shown [10] that when the mean free paths of the gas are equal and if the intermolecular collisions do not affect significantly the density distributions, the flows from the needle are identical for both gases in the collision region. The ratio of the spatial distribution then reduces to:

$$\frac{[\rho(r)]_X}{[\rho(r)]_{ref}} = \frac{N_X}{N_{ref}} \sqrt{\frac{M_X}{M_{ref}}} \tag{2}$$

where N_X, N_{ref} are mass flow rates and M_X, M_{ref} are molecular weights. The mass flow rates and head pressures were adjusted to reproduce as closely as possible the same flow distributions from the needle [10]. In the present study, 1 mbar head pressure for N_2 (0.12 sccm) and 0.9 mbar (0.42 sccm) for THF have been chosen. The absolute elastic differential cross-sections for THF ($DCS_{elas}(E,\theta)_{\mathrm{THF}}$) have been derived from the relative flow formula:

$$\frac{DCS_{elas}(E,\theta)_{\mathrm{THF}}}{DCS_{elas}(E,\theta)_{\mathrm{N}_2}} = \frac{N_e(E,\theta)_{\mathrm{THF}}}{N_e(E,\theta)_{\mathrm{N}_2}} \times \frac{N_{\mathrm{N}_2}}{N_{\mathrm{THF}}} \sqrt{\frac{M_{\mathrm{N}_2}}{M_{\mathrm{THF}}}} \tag{3}$$

where $N_e(E,\theta)_{\mathrm{THF}}$ and $N_e(E,\theta)_{\mathrm{N}_2}$ are the experimentally measured intensities of scattered electrons, M_{THF} and M_{N_2} are molecular weights, N_{THF} and N_{N_2} are mass flow rates and $DCS_{elas}(E,\theta)_{\mathrm{N}_2}$ is the absolute elastic DCS for nitrogen [11].

The experimental set-up in Belgrade is basically the same as reported previously [12] and was slightly upgraded considering acquisition hardware and electron optics. In short, an electron gun produces non monochromated, well collimated electron beam that is crossed perpendicularly by effusive molecular beam, obtained by a nonmagnetic, stainless steel needle. The scattered electrons are retarded and focused by a four-element electrostatic lens into the double mirror cylindrical energy analyzer, followed by a three-element electrostatic zoom lens and a single channel electron multiplier. The electron gun can be rotated around the gas needle from –30° to 120°. It was settled to produce an incident current of about 100 nA. The double μ-metal shield was used to reduce Earth and other stray magnetic fields. The base pressure was about 3×10^{-7} mbar (turbomolecular pump) and the operating pressure was about 6×10^{-6} mbar. Anhydrous THF purchased from Merck KGaA with a stated purity of +99.9% was used after several cycles of freeze-thaw under vacuum. The effective path length correction was found to be negligible in the covered angular range from 25° to 110° (see [13]). The true zero scattering angle was checked according to signal of elastically scattered electrons in the angular range of ±30° around the nominal zero angular position. The uncertainty of the angular scale was found to be less then ±0.5°. Also, the calibration of both angular scale and true zero angular position, as well as reliability of DCS shapes, have been tested according to DCSs for elastic electron-krypton scattering. The latter were obtained immediately before and after measurements in THF, under the same experimental conditions, and showed very good agreement with the most recent results [13–15]. The angular resolution was about ±2°, as confirmed by measurements for Ar and Kr at incident energies where DCSs versus scattering angle reach deep minima. The highest energy resolution was limited by the initial thermal spread of incident electrons to be about 0.5 eV. For the energies above 100 eV, DCSs were usually measured with the resolution of about 1 eV. The accuracy of the incident electron energy was determined to be ±0.5 eV by observing a threshold for He^+ ions yield. Also, the incident energy scale was checked according to deep minima positions in DCSs for Ar and Kr, measured as a function of incident energy and compared to the previous results [16].

On the apparatus in Belgrade, the relative DCSs for a fixed incident electron energy and scattering angle were measured at the maximum of quasielastic peak. The obtained counting rates were normalized by the operating pressure, to avoid influence of small temperature-induced variations of THF vapor pressure. The data acquisition and control of experimental parameters were performed by use of National Instruments multifunctional I/O board, driven by C++ program. In the case of DCS measurements as a function of incident electron energy, a care was taken to ensure constant energy dependent factors (incident beam current, analyzer transmission and detection efficiency). This procedure has been described elsewhere [12,13] and includes tuning of both electron gun and four-element analyzer lens voltages as a function of incident electron energy. As an additional check, the DCSs for Kr were measured as a function of energy immediately after electron-THF measurements, under the same experimental conditions, and compared to previous data [16]. The DCSs were measured as a function of incident energy in two modes — low-energy (40–120 eV) high-resolution (0.5 eV) and high-energy (90–250 eV) low-resolution (1.1 eV) mode, respectively. Then the obtained relative DCSs at the same scattering angle were normalized one to each other at 100 eV.

The final error for relative DCSs measured in Liège includes statistical errors, according to Poisson's distribution, as well as uncertainty of the effective path length correction. The estimated error for the absolute cross-sections for THF obtained by relative flow technique is 25%. This error includes the total error in the measurements of the THF/N_2 DCS ratios, as well as reported total error of absolute DCSs for N_2 [11]. The errors for relative DCSs measured in Belgrade as a function of scattering angle include statistical errors, according to Poisson's distribution and short-term stability errors, according to discrepancy of repeated measurements at the same incident energy and scattering angle. In the case of relative DCSs measured as a function of incident electron energy, in addition to above discussed errors the instability of incident electron beam and transmission function have been accounted, as well. The relative DCSs obtained in Belgrade as a function of scattering angle have been calibrated to the absolute scale according to absolute values obtained by relative flow measurements in Liège and using DCS that was obtained in a separate measurement, as a function of incident energy at a fixed scattering angle. This procedure implies normalization of whole DCS set to a single point and will be explain in detail in the next section. The errors for absolute DCSs account the normalization errors, as well. The latter include both the absolute errors of DCS values measured as a function of incident energy at a fixed scattering angle and uncertainty of the angular scale, which produces the error that is dependent on the shape of a cross-section at particular incident energy (see e.g. [12]).

3 Results and discussion

Firstly, we present a typical vibrational energy loss spectrum of THF, obtained in Liège with high energy resolution (Fig. 2). Note that energy loss region of presented high resolution spectrum is approximately equal to the energy resolution of the spectrometer from Belgrade. The marked vibrational levels in Figure 2 are taken from the recent paper by Lepage et al. [2] (determined by high resolution electron spectroscopy). Due to the lower energy resolution, a larger range of inelastic excitations (vibrational and rotational) contribute to "elastic" DCSs obtained in Belgrade. Therefore, the possibility should be considered whether the lower energy resolution could result in distorted elastic DCS shapes around deep minima, due to the vibrational excitations. According to work on methylamine [8], the vibrational inelastic to elastic intensity ratio decreases drastically with increasing the incident electron energy above 10 eV. Therefore, it should be practically negligible for the energies considered in the present work. Since there is no data for vibrational DCSs for THF molecule, a profound analysis on this effect cannot be done. However, as a simple check, we have measured the contribution of the scattered electron signal in the energy loss regions from 0.1 to 0.45 eV to the overall signal from –0.07 to 0.45 eV, as a function of scattering angle at the

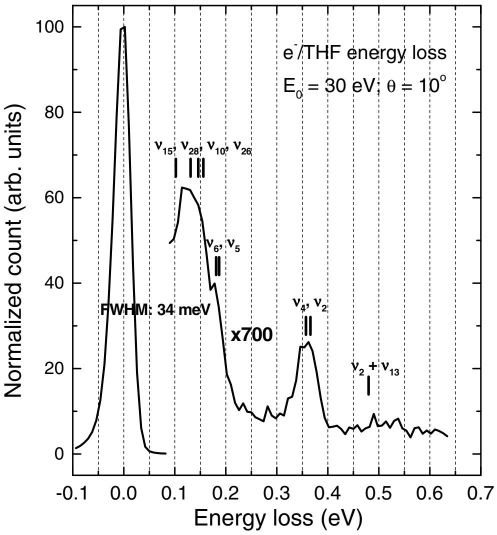

Fig. 2. Energy loss spectrum of THF recorded in Liège at $E_0 = 30$ eV and $\theta = 10^{\circ}$. The marked vibrational states are taken from [2].

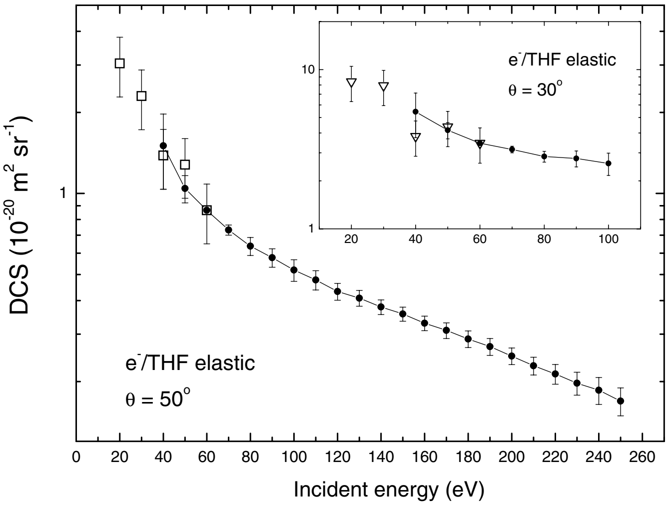

Fig. 3. Energy dependence of absolute DCSs for elastic electron scattering by THF at the scattering angles of 50° and 30° (in the inset). Legend: (▽) absolute DCS values obtained by relative flow measurements; (□) absolute DCS values extracted from DCSs measured as a function of scattering angle and normalized to the absolute scale at 30° with respect to relative flow measurements; (●) DCSs measured as a function of incident electron energy at a fixed scattering angle, and normalized to the absolute scale at 60 eV.

incident electron energy of 30 eV. A very small change of inelastic contribution for the angular region 30−110° was found, which means a negligible influence to the elastic DCS shape. This will be also confirmed below, by comparing DCSs obtained on two different apparata.

The absolute DCS versus incident electron energy for elastic electron scattering by THF at the scattering angle (θ) of 50° is shown in Figure 3. The open squares present results extracted from DCSs obtained as a function of scattering angle and normalized to the absolute scale according to relative flow measurements at 20° and 30° (see the inset in Fig. 3). The full circles present the DCS that is measured directly as a function of incident energy (E_0) in the range 40–250 eV and normalized at 60 eV. A very good agreement can be seen between these two data sets. The 60 eV has been chosen to be the point of calibration because of the smallest uncertainty of relative DCS at this energy, considering the overlapping region. Using the absolute DCS obtained as a function of energy at 50° (Fig. 3), all relative DCSs measured as a function of scattering angle at incident electron energies from 60 eV to 250 eV, have been calibrated to the absolute scale. This scattering angle was chosen as to give the smallest normalization errors and still to be reasonably distant from DCS minima. The DCSs at 20 eV and 30 eV are normalized directly at 30° according to the relative flow measurements. The DCSs in the overlapping region (40 eV and 50 eV) are normalized with respect to the weighted mean of two absolute values at 50°, one extracted from absolute DCS obtained as a function of angle, and the other from absolute DCS obtained as a function of energy (see Fig. 3). Since DCSs were measured versus incident energy up to 250 eV, the relative DCS at 300 eV has been calibrated to the absolute scale according to the ratio of elastic electron scattering signal at 250 eV and 300 eV, obtained under the same experimental conditions, immediately one after the other at 25°.

The absolute DCSs are obtained as a function of scattering angle at the incident electron energies of 20, 30, 40, 50, 60, 70, 80, 90, 100, 120, 150, 170, 200, 220, 250 and 300 eV, in the angular range from 10° to 110° (25° to 110° above 60 eV) with 5° or 10° steps. The results are tabulated in Table 1. The absolute DCSs versus scattering angle at several fixed incident energies are presented in Figure 4, where the results obtained on two different apparata (in Liège and Belgrade, respectively) are compared in the overlapping energy region. Generally, a good agreement of DCS shapes can be seen. A small disagreement at some scattering angles should be the consequence of uncertainty of volume correction, that is more pronounced for higher incident energies (and smaller incident electron beam). However, no systematic difference can be seen that could be described as a consequence of different energy resolutions. Generally, the DCSs show a broad minimum close to 90°, which disappears at about 150 eV and the position of which is weakly dependent on incident electron energy. In the energy range from 30 eV to 300 eV, the absolute DCS value decreases for about order of magnitude. Since there are neither experimental or theoretical results to compare with, we finally note that obtained absolute cross-sections for THF are approximately 3–4 times larger than for methane [17].

4 Conclusion

Elastic scattering of electrons from tetrahydrofuran molecule has been investigated experimentally in the large energy range from 20 eV to 300 eV. The elastic relative DCSs were measured as a function of both scattering angle

Table 1. Experimentally obtained differential cross-sections for elastic electron scattering by tetrahydrofuran molecule in units of 10^{-20} $\mathrm{m^2 sr^{-1}}$ as a function of scattering angle (θ) and incident energy (E_0). The absolute errors (statistical, short-term stability, uncertainty of θ and E_0, uncertainty of incident electron beam and transmission function) in the last significant digits are given in parentheses. The 25% error of absolute DCSs, obtained by relative flow technique and used for normalization to the absolute scale should be accounted, as well.

Θ (o)	E_0 (eV)							
	20	30	40	50	60	70	80	90
10	24.9(6.2)	-	62(32)	112(58)	94(44)	-	-	-
20	16.0(4.0)	19.0(4.5)	17.0(4.2)	18.2(4.6)	12.8(2.9)	-	-	-
25	-	11.29(21)	9.4(2.0)	7.91(94)	6.07(44)	4.62(34)	4.47(43)	4.32(41)
30	8.4(2.1)	7.92(15)	5.3(1.1)	4.50(54)	3.45(25)	2.78(20)	2.65(25)	2.56(24)
35	-	5.34(10)	3.43(74)	3.01(36)	2.29(17)	1.86(14)	1.75(17)	1.68(16)
40	3.61(90)	3.629(69)	2.49(54)	2.09(25)	1.57(11)	1.313(96)	1.21(12)	1.15(11)
45	-	2.605(53)	1.84(40)	1.50(18)	1.137(83)	0.975(72)	0.864(83)	0.797(76)
50	3.04(76)	2.017(44)	1.44(31)	1.16(14)	0.866(63)	0.731(54)	0.637(61)	0.577(55)
55	-	1.654(36)	1.15(25)	0.90(11)	0.649(47)	0.553(41)	0.483(46)	0.463(44)
60	1.90(38)	1.383(30)	0.96(21)	0.690(82)	0.486(36)	0.442(33)	0.401(39)	0.381(36)
65	-	1.147(26)	0.79(17)	0.536(64)	0.386(28)	0.373(27)	0.340(33)	0.318(30)
70	1.53(38)	0.938(22)	0.62(13)	0.425(51)	0.324(24)	0.317(23)	0.277(27)	0.253(24)
75	-	0.771(19)	0.51(11)	0.365(43)	0.287(21)	0.271(20)	0.227(22)	0.202(19)
80	1.27(41)	0.657(17)	0.419(90)	0.323(39)	0.251(18)	0.230(17)	0.192(19)	0.176(17)
85	-	0.593(16)	0.387(83)	0.291(35)	0.220(16)	0.204(15)	0.172(17)	0.158(15)
90	1.07(44)	0.562(15)	0.367(79)	0.263(31)	0.203(15)	0.196(14)	0.171(16)	0.158(15)
95	-	0.549(15)	0.353(76)	0.250(30)	0.199(15)	0.204(15)	0.177(17)	0.168(16)
100	1.72(83)	0.550(15)	0.370(80)	0.259(31)	0.212(16)	0.224(17)	0.201(19)	0.189(18)
105	-	0.585(16)	0.401(86)	0.284(34)	0.241(18)	0.263(19)	0.233(22)	0.216(21)
110	-	0.667(18)	0.47(10)	0.337(40)	0.281(21)	0.306(23)	0.266(26)	0.246(23)

Θ (o)	E_0 (eV)							
	100	120	150	170	200	220	250	300
25	3.92(43)	3.06(28)	2.27(22)	1.81(17)	1.59(16)	1.46(16)	1.23(18)	0.99(18)
30	2.33(25)	1.88(17)	1.39(13)	1.10(10)	0.938(94)	0.848(95)	0.73(11)	0.62(12)
35	1.51(17)	1.19(11)	0.867(83)	0.694(63)	0.601(61)	0.561(63)	0.510(75)	0.456(85)
40	1.02(11)	0.784(73)	0.585(56)	0.512(47)	0.469(47)	0.437(49)	0.385(57)	0.310(58)
45	0.712(78)	0.551(51)	0.441(42)	0.406(37)	0.352(35)	0.311(35)	0.258(38)	0.189(35)
50	0.520(57)	0.432(40)	0.357(34)	0.310(28)	0.249(25)	0.214(24)	0.169(25)	0.136(25)
55	0.426(47)	0.356(33)	0.266(25)	0.221(20)	0.172(17)	0.147(17)	0.126(19)	0.112(21)
60	0.353(39)	0.275(26)	0.193(18)	0.166(15)	0.135(14)	0.122(14)	0.111(16)	0.093(17)
65	0.280(31)	0.209(19)	0.153(15)	0.136(12)	0.117(12)	0.110(12)	0.095(14)	0.074(14)
70	0.219(24)	0.163(15)	0.126(12)	0.123(11)	0.108(11)	0.097(11)	0.080(12)	0.064(12)
75	0.175(19)	0.137(13)	0.118(11)	0.116(11)	0.0941(95)	0.0838(95)	0.068(10)	0.056(11)
80	0.159(18)	0.130(12)	0.113(11)	0.110(10)	0.0853(86)	0.0731(83)	0.0605(89)	0.0472(88)
85	0.149(16)	0.124(12)	0.108(10)	0.1030(94)	0.0779(79)	0.0672(76)	0.0545(81)	0.0417(78)
90	0.150(16)	0.125(12)	0.106(10)	0.0959(88)	0.0733(74)	0.0626(71)	0.0507(75)	0.0392(73)
95	0.159(18)	0.134(13)	0.1003(96)	0.0931(85)	0.0703(71)	0.0583(66)	0.0466(69)	0.0374(70)
100	0.171(19)	0.136(13)	0.1012(97)	0.0923(85)	0.0674(68)	0.0555(63)	0.0446(66)	0.0344(64)
105	0.191(21)	0.138(13)	0.1010(97)	0.0930(85)	0.0645(65)	0.0551(63)	0.0441(65)	0.0328(61)
110	0.210(23)	0.149(14)	0.104(10)	0.0930(85)	0.0652(66)	0.0536(61)	0.0432(64)	0.0297(56)

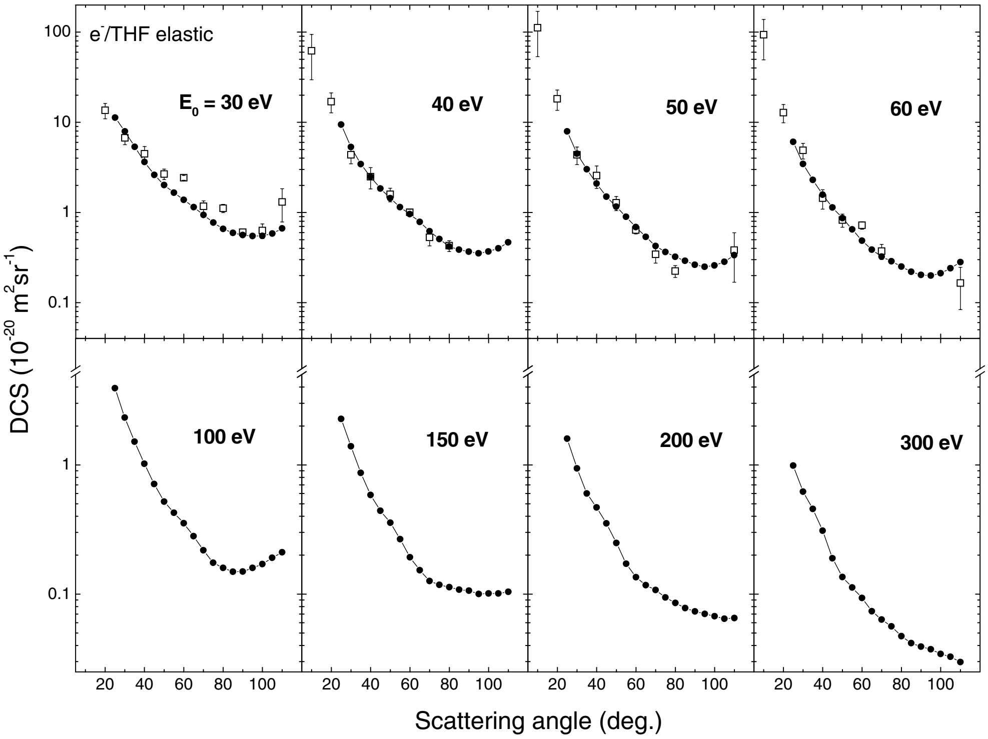

Fig. 4. Angular dependence of absolute DCSs for elastic electron scattering by THF at different fixed incident energies. (□) Results obtained in Liège; (●) results obtained in Belgrade.

and incident electron energy. The relative flow technique has been used for calibration of obtained data set to the absolute scale. The DCSs were measured on two different experimental systems, with high and low energy resolution, respectively, and obtained results are compared. Also, the vibrational energy loss spectrum was presented and influence of inelastic excitation to elastic DCS shapes has been discussed. DCSs are tabulated in order to facilitate further model simulations of low(medium)-energy electron interaction with molecules of biological interest.

We are very grateful to Dr. J. Jureta for his help on experimental work. This work was supported by European Cooperation in the field of Scientific and Technical Research, Action P9 Radiation Damage in Biomolecular Systems. Part of the authors (A.M., D.Š. and B.M.) are also grateful for the support of Ministry of Science and Environmental Protection of Republic of Serbia under project OI1424. The Patrimoine of the University of Liège, the Fonds National de la Recherche Scientifique and the Fonds de la Recherche Fondamentale Collective have supported this research. M.-J. H.-F. wishes to acknowledge the Fonds National de la Recherche Scientifique for a position.

References

1. B. Boudaïffa, P. Cloutier, D. Hunting, M.A. Huels, L. Sanche, Science **287**, 1658 (2000)
2. M. Lepage, S. Letarte, M. Michaud, F. Motte-Tollet, M.-J. Hubin-Franskin, D. Roy, L. Sanche, J. Chem. Phys. **109**, 5980 (1998)
3. D. Antic, L. Parenteau, M. Lepage, L. Sanche, J. Phys. Chem. B **103**, 6611 (1999)
4. D. Antic, L. Parenteau, L. Sanche, J. Phys. Chem. B **104**, 4711 (2000)
5. S.-P. Breton, M. Michaud, C. Jäggle, P. Swiderek, L. Sanche, J. Chem. Phys. **121**, 11240 (2004)
6. A. Roldán, J.M. Pérez, A. Williart, F. Blanco, G. Garcia, J. Appl. Phys. **95(10)**, 5865 (2004)
7. U. Titt, V. Dangendorf, B. Grosswendt, H. Schuhmacher, Nucl. Instr. Meth. A **477**, 536 (2002)
8. F. Motte-Tollet, M.J. Hubin-Franskin, J.E. Collin, J. Chem. Phys. **97(10)**, 7314 (1992); F. Motte-Tollet, J. Heinesch, J.M. Gingell, N.J. Mason, J. Chem. Phys. **106**, 5990 (1997)
9. S. Trajmar, D.F. Register, A. Chutjian, Phys. Rep. **97**, 219 (1983)
10. J.C. Nickel, P.W. Zetner, G. Shen, S. Trajmar, J. Phys. E **22**, 730 (1989)
11. J.C. Nickel, C. Mott, I. Kanik, D.C. McCollum, J. Phys. B: At. Mol. Opt. Phys. **21**, 1867 (1988)
12. A.R. Milosavljević, S. Telega, D. Šević, J.E. Sienkiewicz, B.P. Marinković, Eur. Phys. J. D **29**, 329 (2004)
13. A.R. Milosavljević, V.I. Kelemen, D.M. Filipović, S.M. Kazakov, V. Pejčev, D. Šević, B.P. Marinković, J. Phys. B: At. Mol. Opt. Phys. **38**, 2195 (2005)
14. H. Cho, R.P. McEachran, H. Tanaka, S.J. Buckman, J. Phys. B: At. Mol. Opt. Phys. **37**, 4639 (2004)
15. A. Danjo, J. Phys. B: At. Mol. Opt. Phys. **21**, 3759 (1988)
16. D. Cvejanović, D.A. Crowe, J. Phys. B: At. Mol. Opt. Phys. **30**, 2873 (1997)
17. L. Boesten, H. Tanaka, J. Phys. B: At. Mol. Opt. Phys. **24**, 821 (1991)